

Emergence of dynamic instability by hybridizing synthetic self-assembled dipeptide fibers with surfactant micelles

Shogo Torigoe,¹ Kazutoshi Nagao,¹ Ryou Kubota,^{1*} Itaru Hamachi^{1,2*}

¹Department of Synthetic Chemistry and Biological Chemistry, Graduate School of Engineering, Kyoto University, Katsura, Nishikyo-ku, Kyoto 615-8510, Japan. ²JST-ERATO, Hamachi Innovative Molecular Technology for Neuroscience, Kyoto University, Katsura, Nishikyo-ku, Kyoto 615-8530, Japan.

ABSTRACT: Supramolecular chemistry currently faces the challenge of controlling nonequilibrium dynamics, such as the dynamic instability of microtubules. In this study, we explored the emergence of dynamic instability through the hybridization of peptide-type supramolecular nanofibers with surfactant micelles. Using real-time confocal imaging, we discovered that the addition of micelles to nanofibers induced the simultaneous but asynchronous growth and shrinkage of nanofibers, during which the total number of fibers decreased monotonically. This dynamic phenomenon unexpectedly persisted for 6 days and was driven not by chemical reactions but by noncovalent supramolecular interactions between peptide-type nanofibers and surfactant micelles. This study demonstrates a strategy for inducing autonomous supramolecular dynamics, which will open up possibilities for developing soft materials applicable to biomedicine and soft robotics.

Having explored self-assembly in the thermodynamic stable state, supramolecular chemistry now confronts the challenge of controlling nonequilibrium dynamics.^{1–21} Chemically driven nonequilibrium systems, including feedbacks, waves, and oscillations, hold the key to fabricating active soft materials equipped with cell-inspired features, such as autonomous motility and spatiotemporally regulated hierarchical structures.^{22–25} The dynamic instability of microtubules represents one of the intriguing dynamics occurring in cells, mainly driven by the energy dissipation of guanosine 5'-triphosphate.²⁶ Microtubules abruptly transition between growth and shrinkage, allowing the coexistence of growing and shrinking fibers even in a uniform subunit concentration; the systems exhibiting both two characteristics are termed as the dynamic instability.²⁷ In synthetic self-assemblies, equilibrium dynamics are commonly observed, and their kinetics rely on the energy barrier between assembly and disassembly. However, synthetic supramolecular nanofibers generally lack autonomous switching between growth and shrinkage during (de)polymerization.²⁸ To date, several researchers have successfully demonstrated the coexistence of growing and shrinking nanofibers through microscopic observations, mostly with experimental setups using spatial gradients.^{11,29–37} Although fuel-driven dissipative self-assemblies have been intensively developed over the past decade,^{38–50} there is still a limited number of examples of these assemblies exhibiting dynamic instability-like behavior.³⁰ It is thus indispensable to develop a novel, simple supramolecular strategy for realizing synthetic molecules exhibiting dynamic instability.

Here, we report the emergence of dynamic instability through the hybridization of peptide-type supramolecular nanofibers with surfactant micelles composed of sodium dodecyl sulfate

(SDS) (Figure 1a). Using time-lapse confocal laser scanning microscopic (CLSM) imaging to visualize the system, we found that the total number of fibers decreased monotonically upon the addition of SDS micelles. Moreover, growth and shrinkage of nanofibers occurred concurrently, and the periods of growth and shrinkage were not synchronized among nanofibers, similar to the dynamic instability of microtubules. This dynamic behavior unexpectedly persisted for 6 days and was driven by noncovalent interactions between the nanofibers and SDS micelles. A series of control experiments suggested that both the hydrophobic interior of SDS micelles and the dynamic equilibrium between micelles and monomers were crucial for this dynamic behavior. Our study demonstrates a novel approach for designing autonomous nonequilibrium systems through synthetic supramolecular chemistry.

A diphenylalanine derivative with a benzyloxime group at the *N*-terminus (Ox, Figure 1a) was employed as the peptide-type hydrogelator.³³ The Ox peptide self-assembles into one-dimensional nanofibrous structures, mainly driven by hydrogen bonding and π - π interactions. CLSM was used to monitor fiber formation resulting from *in situ* oxime formation through the reaction between an aldehyde-tethered dipeptide precursor (Ald) and *O*-benzylhydroxylamine in an aqueous buffer containing a fluorescent probe (Figure S1). Real-time CLSM showed that fiber formation was initiated stochastically in time and space after an induction time of approximately 7 min, and nanofibers grew gradually over 30 min (Movie 1). In addition, some of the fibers grew on the end of Ox peptide fragments, suggesting that the mechanism of growth was nucleation–elongation (Figure S2, Movie 2). During this time, shrinkage of nanofibers was negligible.

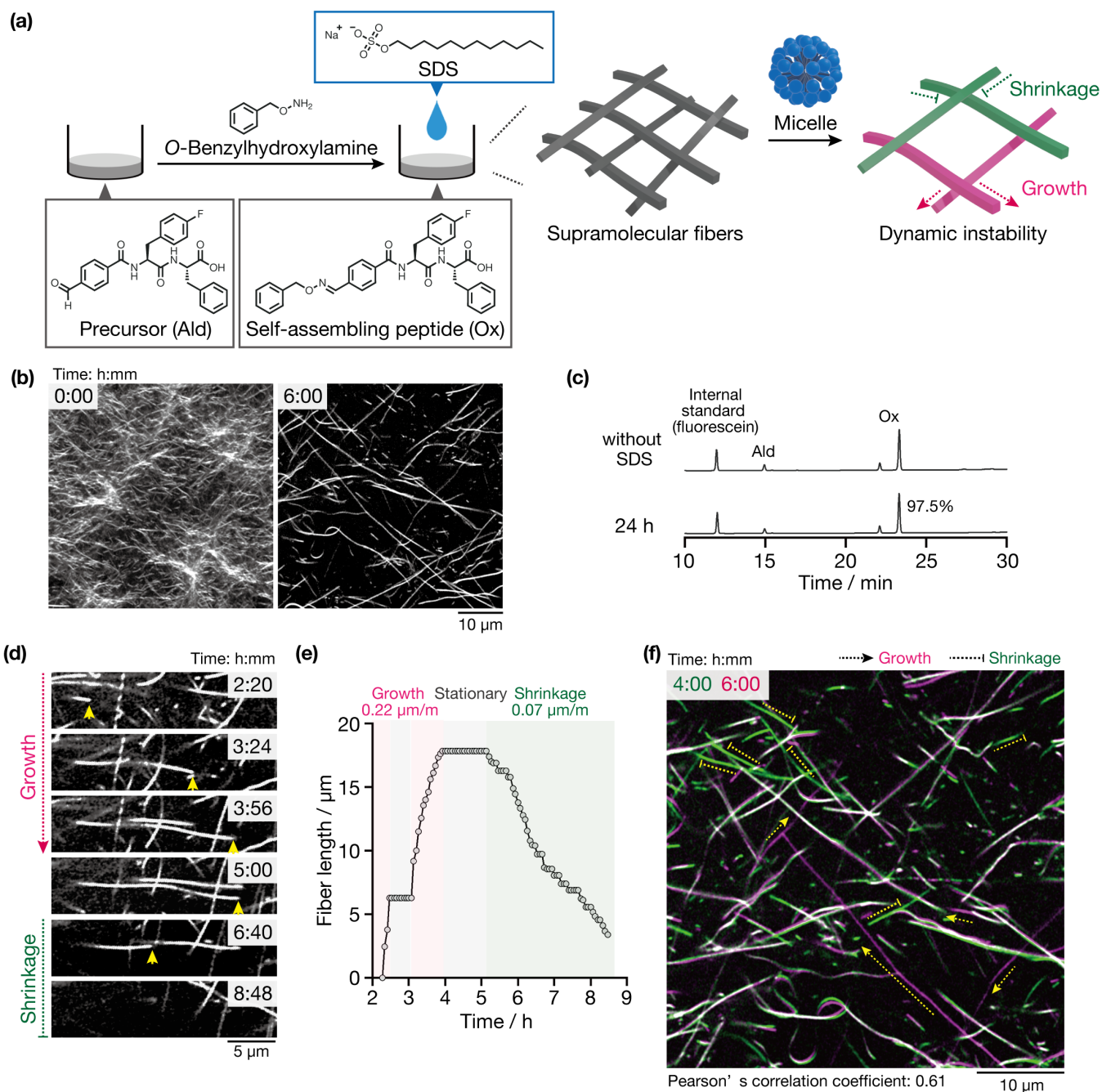


Figure 1. (a) Emergence of dynamic instability by hybridizing synthetic supramolecular fibers with surfactant micelles. (b) CLSM images and (c) HPLC charts before and after addition of SDS micelles. (d) CLSM images and (e) time course of single fiber dynamics. (f) Overlay of CLSM images at different time points (green: 4 h, magenta: 6 h). Condition: [Ald] = 3.6 mM, [O-benzylhydroxylamine] = 3.6 mM, [SDS] = 5.0 mM, [fluorescent probe] = 4.0 μ M in 100 mM MES, pH 7.0, 30 $^{\circ}$ C.

To induce nanofiber degradation, we hybridized the Ox nanofibers with SDS micelles. SDS micelles have hydrophobic interiors, and the monomer and micellar assembly are known to be in dynamic equilibrium.⁵¹ We anticipated that the inner core of the SDS micelles interacts with Ox nanofibers through hydrophobic interactions, leading to nanofiber decomposition. We also considered the possibility that electrostatic repulsion between anionic SDS and anionic Ox peptide suppresses rapid fiber decomposition, thereby allowing sufficient time for the system to reach the thermodynamic equilibrium state.

We initially examined whether SDS micelles interacted with Ox nanofibers using CLSM. A solution containing SDS

micelles (5.0 mM, critical micelle concentration (CMC) of 1.5 mM, Figure S3) was added to an Ox hydrogel (93% of the Ald precursor was converted to the Ox peptide, Figure S4). CLSM imaging showed that the Ox nanofibers were relatively short, straight, and entangled before the addition of SDS micelles (Figure 1b left). In contrast, the addition of SDS micelles markedly reduced the number of nanofibers and altered the fiber morphology, from linear to longer curved fibers (Figure 1b right, Figure S5). Histogram analysis indicated that the fiber length was distributed around 3.5 and 8.9 μ m (average fiber length) before and after the addition of SDS micelles, respectively (Figure S6). These results indicated that Ox nanofibers and SDS

micelles indeed interacted with each other and that these interactions induced degradation of the original nanofibers and re-growth of nanofibers with different morphologies. Surprisingly, time-lapse CLSM imaging showed that these nanofibers exhibited autonomous growth and shrinkage behaviors (Figure 1d). As shown in Figure 1e, for example, a fiber grew over 1.6 μm (from 2 h 20 min to 3 h 56 min) with an average rate of 0.22 $\mu\text{m}/\text{min}$, and then after a lag time of 1 h (the stationary phase), the grown fiber abruptly shrank over 3 h with an average rate of 0.07 $\mu\text{m}/\text{min}$. Both growing and shrinking fibers were observed in the same field of view, and the growth and shrinkage of fibers were not synchronized in time and space (Figure 1f). 4D CLSM movie clearly visualized that fiber growth and shrinkage indeed occurred, rather than fiber inflow and outflow (Movie 3). High-performance liquid chromatography (HPLC) analysis confirmed that the Ox peptide did not decompose during incubation, which suggested that autonomous growth and shrinkage were not driven by chemical reactions, in contrast to previous dissipative self-assembly (Figure 1c). Overall, hybridization of Ox nanofibers with SDS micelles was characterized by nonequilibrium dynamics, similar to the dynamic instability of naturally occurring microtubules. Hereafter, we refer to this nonequilibrium dynamics as synthetic dynamic instability.

To investigate synthetic dynamic instability in detail, a time-lapse CLSM movie was acquired for 12 h after the addition of SDS micelles (Figure 2a, Movie 4). Shrinkage of the initial Ox nanofibers began 4 min after the addition of SDS micelles, and concurrently, a small number of short new nanofibers grew from the edge of the original fibers (Figure S7). From 20 min, small new aggregates grew from their ends, independently of preexisting nanofibers. The newly formed fibers also shrank after a lag time. After 1 h, almost all of the original nanofibers were degraded and replaced by regrown nanofibers. Autonomous growth and shrinkage persisted even after 12 h. Quantitative analyses revealed a monotonic decrease in the total number of nanofibers over time (Figure 2b, S8). According to single-fiber tracking analysis, the growing and shrinking rates of each fiber varied, and at 3 h, the average growing and shrinking rates were 0.3 ± 0.2 and 0.22 ± 0.17 $\mu\text{m}/\text{min}$, respectively, which were comparable with and slightly slower than those of microtubules *in vitro*, respectively (Figure 2c, S9).⁵² Notably, the distribution of growing and shrinking rates remained similar at 3, 6, and 12 h, although the frequency of growth and shrinkage gradually decreased (Figure S10). Observations of long-term incubation showed that fiber growth and shrinkage occurred on day 6, and few fibers, which did not exhibit dynamics, remained after day 7 (Figure S11, Movie 5). Overall, synthetic dynamic instability was driven by noncovalent interactions between the Ox peptide and SDS and persisted for 6 days until the system reached the thermodynamically stable state.

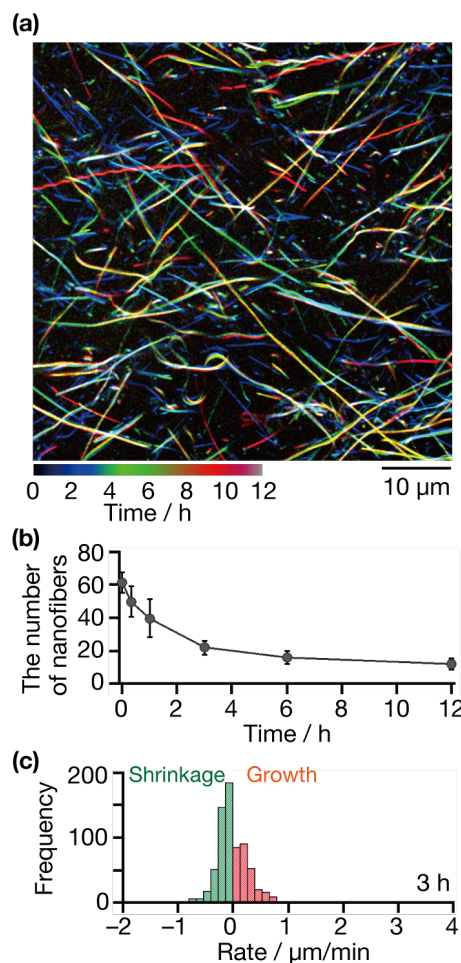


Figure 2. (a) Overlay of time-series CLSM images using a temporal color code. (b) Time course of the number of nanofibers. The data represent the mean \pm standard deviation ($n = 4$). (c) Histogram analysis of the growth and shrinkage rate at 3 h. The shrinkage rate was shown as a negative value.

Quantitative analyses revealed three unique dynamics of nanofiber growth and shrinkage. The first is oscillation-like repetition (Figure 3a, Movie 6). From 10 h 48 min to 11 h 4 min, a very short aggregate grew to 9.3 μm mainly at the right end with an average rate of 0.52 $\mu\text{m}/\text{min}$. Then, the fiber gradually shrank to 1.0 μm over 32 min (0.26 $\mu\text{m}/\text{min}$) and regrew to 12 μm over 16 min (0.70 $\mu\text{m}/\text{min}$), accompanied with a temporary shrinking period. The second is treadmilling-like dynamics, which is one of the representative nonequilibrium dynamics of actin filaments (Figure 3b). A short nanofiber gradually grew from its left end (red arrow) to the left side of the field of view, and the same nanofiber concurrently shrank from its other end (green arrow), resulting in treadmilling-like dynamics. The growth rate (0.47 $\mu\text{m}/\text{min}$) was higher than the shrinking rate (0.31 $\mu\text{m}/\text{min}$), and thus the total fiber length eventually increased from 2.71 to 15.55 μm over 1.3 h. In the third case, shrinkage of a few fibers was initiated at the middle of the fiber. Specifically, a grown fiber broke at its mid-point, and shrinkage started from one end but not from the other end (Figure S12).

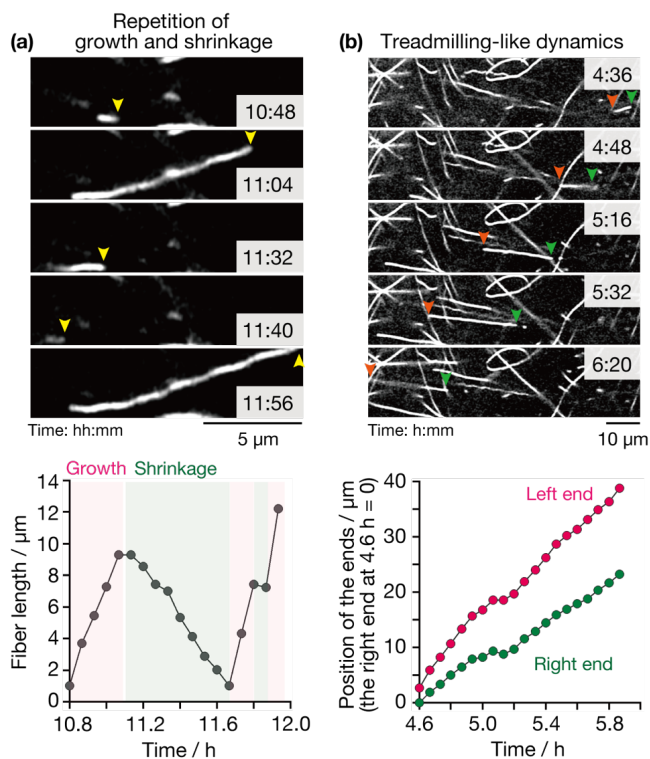


Figure 3. (Top) Unique dynamic behaviors and (bottom) quantitative analysis of the growing and shrinking fibers. (a) Repetition of growth and shrinkage. (b) Treadmilling-like behavior.

The dependence of autonomous growth/shrinkage on SDS micelles was investigated by varying the concentration of SDS. When SDS was added at concentrations below CMC (0.50 mM), neither growth nor shrinkage proceeded until at least 12 h, which was also confirmed with quantitative single-fiber analysis (Figure S13). From these results, we concluded that the interactions between the SDS monomer and Ox nanofibers were too weak to induce fiber shrinkage. In contrast, when an excess amount of SDS was added (50 mM), fiber shrinkage was dominant and proceeded within 20 min, while fiber regrowth was negligible (Figure S14). The resultant phase diagram revealed that our synthetic dynamic instability emerged in the rather wide concentration ranges of SDS and the Ox peptide (Figure 4, Movie 7–9). Interestingly, fiber growth and shrinkage were negligible when a liposome solution (96:4 1,2-dioleoyl-*sn*-glycero-3-phosphocholine/1,2-distearoyl-*sn*-glycero-3-phosphate) was added instead of SDS micelles (Figure S15). These results indicated that both the hydrophobic environment provided by SDS micelles and the dynamic equilibrium between SDS micelles and monomers were critically important for synthetic dynamic instability.

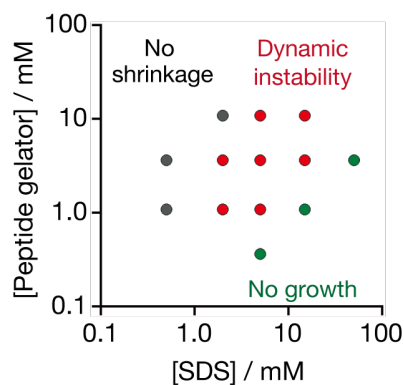


Figure 4. Phase diagram as a function of concentrations of the peptide hydrogelator and SDS.

From the above results, we propose the following mechanism of synthetic dynamic instability (Figure 5). After the addition of SDS micelles to Ox nanofibers, SDS micelles interact with nanofibers, mainly at their hydrophobic ends. The inner hydrophobic environment of SDS micelles induces the disassembly of Ox nanofibers into Ox short peptide aggregates, leading to nanofiber shrinkage from the end. Subsequently, some of the decomposed short peptide aggregates are released from the SDS micelles owing to the dynamics of SDS micelles, and these released aggregates/peptides function as seeds and active monomers to initiate nanofiber regrowth. Furthermore, SDS micelles interact with the regrown nanofibers at their tips to induce fiber shrinkage, as in the case of the original Ox nanofibers. The observation of a stationary phase between the growth and shrinkage phases indicates the existence of an energy barrier, which likely arises from electrostatic repulsion between SDS micelles and nanofibers. As these processes repeat, Ox peptides become trapped within SDS micelles, which gradually attenuates the growth and shrinkage dynamics of the nanofibers, leading to thermodynamic equilibrium after 7 days.

To date, several researchers have observed the nonequilibrium dynamics of supramolecular fibers, including the coexistence of growth and shrinkage (Table S1), using spatial concentration gradients,³¹ localized photo-control,³⁴ and/or external fields³⁷ (including repetitive/continuous supply of chemical/electrical fuels). Marangoni flows were recently reported to drive autonomous fiber growth and shrinkage through the surface tension gradient, although these processes currently require source droplets and are limited to the interface.^{32,35} Moreover, van Esch and coworkers used chemical reaction-driven dissipative self-assembly to realize out-of-equilibrium dynamics, similar to dynamic instability.³⁰ In contrast to these previous studies, our system is unique in that autonomous growth and shrinkage of peptide-based nanofibers, persisting over 6 days, can be driven by noncovalent (supramolecular) interactions without an elaborate experimental setup. Two factors would be crucial for the emergence of synthetic dynamic instability: (i) distinct mechanisms on the fiber growth and shrinkage, (ii) a delicate balance of supramolecular interactions between peptide fibers/aggregates and SDS micelles. Owing to the simplicity of our system, we believe that further extension, such as equipment to elicit stimulus responses, will allow control of synthetic dynamic instability in space and time. It is envisioned that harnessing this type of autonomous supramolecular dynamics will provide opportunities for the development of intelligent materials with potential applications in biomedicine and soft robotics.

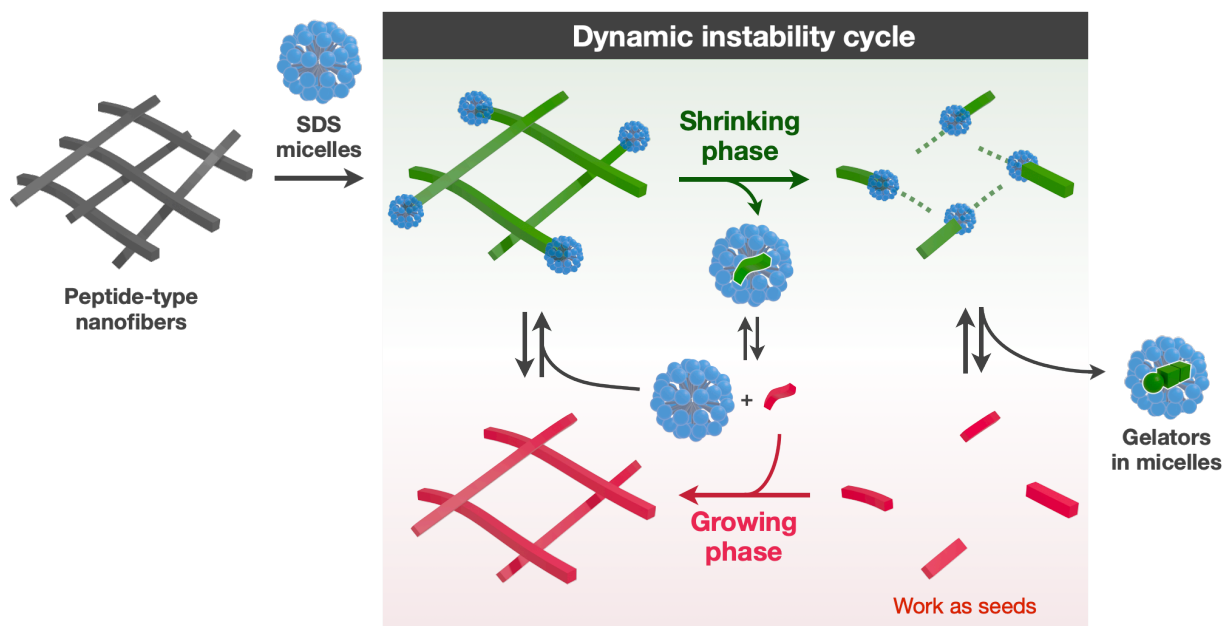


Figure 5. Plausible mechanism of synthetic dynamic instability of supramolecular nanofibers and surfactant micelles. Interaction strength between peptide fibers/aggregates and SDS micelles may be dependent on the fiber length, so that some of peptide aggregates are released from micelles followed by the fiber regrowth.

ASSOCIATED CONTENT

Supporting Information

The Supporting Information is available free of charge on the ACS Publications website.

Description of materials, experimental methods, chemical structures of the fluorescent probes; HPLC analyses and time-lapse CLSM images of *in situ* oxime formation; determination of the critical micelle concentration of SDS by uptake of Nile red; Quantitative analyses of the fiber length, curvature, and number; time-dependent CLSM observation over 7 days; tracking of growing and shrinking fibers; histogram analysis of the growth and shrinkage rates; time-lapse CLSM imaging upon addition of various concentrations of SDS and addition of liposome (PDF).

Formation process of Ox nanofibers through *in situ* oxime generation without seeds. Condition: [Ald] = 3.9 mM, [*O*-benzylhydroxylamine] = 3.9 mM, [fluorescent probe] = 4.0 μ M in 100 mM MES, pH 7.0, at 30 $^{\circ}$ C (MP4).

Formation process of Ox nanofibers through *in situ* oxime generation with seeds. Condition: [Ald] = 1.9 mM, [*O*-benzylhydroxylamine] = 1.9 mM, [fluorescent probe] = 4.0 μ M in 100 mM MES, pH 7.0, at 30 $^{\circ}$ C (MP4).

4D CLSM movie of synthetic dynamic instability of the nanofibers 4 h after addition of SDS micelles. Condition: [Ald] = 3.6 mM, [*O*-benzylhydroxylamine] = 3.6 mM, [SDS] = 5.0 mM, [fluorescent probe] = 4.0 μ M in 100 mM MES, pH 7.0 at 30 $^{\circ}$ C (MP4).

Time-lapse CLSM movie of synthetic dynamic instability of the nanofibers immediately after addition of SDS micelles. Condition: [Ald] = 3.6 mM, [*O*-benzylhydroxylamine] = 3.6 mM, [SDS] = 5.0

mM, [fluorescent probe] = 4.0 μ M in 100 mM MES, pH 7.0 at 30 $^{\circ}$ C (MP4).

Time-dependence of synthetic dynamic instability of the nanofibers from day 1 to 7 after addition of SDS micelles. Condition: [Ald] = 3.6 mM, [*O*-benzylhydroxylamine] = 3.6 mM, [SDS] = 5.0 mM, [fluorescent probe] = 4.0 μ M in 100 mM MES, pH 7.0 at 30 $^{\circ}$ C (MP4).

Unique dynamic behaviors during synthetic dynamic instability (MP4).

Concentration dependence of Ox and SDS on dynamic instability. Condition: [Ald] = 1.1 mM, [*O*-benzylhydroxylamine] = 1.1 mM, [SDS] = 2.0, 5.0, 15 mM, [fluorescent probe] = 4.0 μ M in 100 mM MES, pH 7.0 at 30 $^{\circ}$ C (MP4).

Concentration dependence of Ox and SDS on dynamic instability. Condition: [Ald] = 3.6 mM, [*O*-benzylhydroxylamine] = 3.6 mM, [SDS] = 2.0, 15, 50 mM, [fluorescent probe] = 4.0 μ M in 100 mM MES, pH 7.0 at 30 $^{\circ}$ C (MP4).

Concentration dependence of Ox and SDS on dynamic instability. Condition: [Ald] = 11 mM, [*O*-benzylhydroxylamine] = 11 mM, [SDS] = 5.0, 15 mM, [fluorescent probe] = 4.0 μ M in 100 mM MES, pH 7.0 at 30 $^{\circ}$ C (MP4).

AUTHOR INFORMATION

Corresponding Authors

Itaru Hamachi – Department of Synthetic Chemistry and Biological Chemistry, Graduate School of Engineering, Kyoto University, Katsura, Nishikyo-ku, Kyoto 615-8510, Japan; JST-ERATO,

Hamachi Innovative Molecular Technology for Neuroscience, Kyoto University, Katsura, Nishikyo-ku, Kyoto 615-8530, Japan; orcid.org/0000-0002-3327-3916; Email:

ihamachi@sbchem.kyoto-u.ac.jp

Ryou Kubota – Department of Synthetic Chemistry and Biological Chemistry, Graduate School of Engineering, Kyoto University, Katsura, Nishikyo-ku, Kyoto 615-8510, Japan; orcid.org/0000-0001-8112-8169; Email: rkubota@sbchem.kyoto-u.ac.jp

Authors

Shogo Torigoe – Department of Synthetic Chemistry and Biological Chemistry, Graduate School of Engineering, Kyoto University, Katsura, Nishikyo-ku, Kyoto 615-8510, Japan

Kazutoshi Nagao – Department of Synthetic Chemistry and Biological Chemistry, Graduate School of Engineering, Kyoto University, Katsura, Nishikyo-ku, Kyoto 615-8510, Japan

Notes

The authors declare no competing interests.

ACKNOWLEDGMENT

We appreciate Prof. Kenji Matsuda (Kyoto University) for his support in DLS measurement. This work was supported by the Japan Science and Technology Agency (JST) ERATO Grant Number JPMJER1802 to I.H., and by a Grant-in-Aid for Scientific Research (B) (JSPS KAKENHI Grant JP22H02195) to R.K. We thank Edanz (<https://jp.edanz.com/ac>) for editing a draft of this manuscript.

REFERENCES

- (1) Aida, T.; Meijer, E. W.; Stupp, S. I. Functional Supramolecular Polymers. *Science* **2012**, *335*, 813–817.
- (2) Lehn, J.-M. Perspectives in Chemistry--Aspects of Adaptive Chemistry and Materials. *Angew. Chem. Int. Ed.* **2015**, *54*, 3276–3289.
- (3) Ashkenasy, G.; Hermans, T. M.; Otto, S.; Taylor, A. F. Systems Chemistry. *Chem. Soc. Rev.* **2017**, *46*, 2543–2554.
- (4) Das, K.; Gabrielli, L.; Prins, L. J. Chemically Fueled Self-Assembly in Biology and Chemistry. *Angew. Chem. Int. Ed.* **2021**, *60*, 20120–20143.
- (5) Korevaar, P. A.; George, S. J.; Markvoort, A. J.; Smulders, M. M. J.; Hilbers, P. A. J.; Schenning, A. P. H. J.; De Greef, T. F. A.; Meijer, E. W. Pathway Complexity in Supramolecular Polymerization. *Nature* **2012**, *481*, 492–496.
- (6) Boekhoven, J.; Koot, M.; Wezendonk, T. A.; Eelkema, R.; van Esch, J. H. A Self-Assembled Delivery Platform with Post-Production Tunable Release Rate. *J. Am. Chem. Soc.* **2012**, *134*, 12908–12911.
- (7) Ogi, S.; Sugiyasu, K.; Manna, S.; Samitsu, S.; Takeuchi, M. Living Supramolecular Polymerization Realized through a Biomimetic Approach. *Nat. Chem.* **2014**, *6*, 188–195.
- (8) Kang, J.; Miyajima, D.; Mori, T.; Inoue, Y.; Itoh, Y.; Aida, T. A Rational Strategy for the Realization of Chain-Growth Supramolecular Polymerization. *Science* **2015**, *347*, 646–651.
- (9) Wilson, M. R.; Solà, J.; Carlone, A.; Goldup, S. M.; Lebrasseur, N.; Leigh, D. A. An Autonomous Chemically Fuelled Small-Molecule Motor. *Nature* **2016**, *534*, 235–240.
- (10) Maiti, S.; Fortunati, I.; Ferrante, C.; Scrimin, P.; Prins, L. J. Dissipative Self-Assembly of Vesicular Nanoreactors. *Nat. Chem.* **2016**, *8*, 725–731.
- (11) Aliprandi, A.; Mauro, M.; De Cola, L. Controlling and Imaging Biomimetic Self-Assembly. *Nat. Chem.* **2016**, *8*, 10–15.
- (12) Ikegami, T.; Kageyama, Y.; Obara, K.; Takeda, S. Dissipative and Autonomous Square-Wave Self-Oscillation of a Macroscopic Hybrid Self-Assembly under Continuous Light Irradiation. *Angew. Chem. Int. Ed.* **2016**, *55*, 8239–8243.
- (13) Fukui, T.; Uchihashi, T.; Sasaki, N.; Watanabe, H.; Takeuchi, M.; Sugiyasu, K. Direct Observation and Manipulation of Supramolecular Polymerization by High-Speed Atomic Force Microscopy. *Angew. Chem. Int. Ed.* **2018**, *57*, 15465–15470.
- (14) Morrow, S. M.; Colomer, I.; Fletcher, S. P. A Chemically Fuelled Self-Replicator. *Nat. Commun.* **2019**, *10*, 1011.
- (15) Chen, R.; Neri, S.; Prins, L. J. Enhanced Catalytic Activity under Non-Equilibrium Conditions. *Nat. Nanotechnol.* **2020**, *15*, 868–874.
- (16) Korevaar, P. A.; Kaplan, C. N.; Grinthal, A.; Rust, R. M.; Aizenberg, J. Non-Equilibrium Signal Integration in Hydrogels. *Nat. Commun.* **2020**, *11*, 386.
- (17) Monreal Santiago, G.; Liu, K.; Browne, W. R.; Otto, S. Emergence of Light-Driven Protometabolism on Recruitment of a Photocatalytic Cofactor by a Self-Replicator. *Nat. Chem.* **2020**, *12*, 603–607.
- (18) Bian, T.; Gardin, A.; Gemen, J.; Houben, L.; Perego, C.; Lee, B.; Elad, N.; Chu, Z.; Pavan, G. M.; Klajn, R. Electrostatic Co-Assembly of Nanoparticles with Oppositely Charged Small Molecules into Static and Dynamic Superstructures. *Nat. Chem.* **2021**, *13*, 940–949.
- (19) Samperi, M.; Bdiri, B.; Sleet, C. D.; Markus, R.; Mallia, A. R.; Pérez-García, L.; Amabilino, D. B. Light-Controlled Micron-Scale Molecular Motion. *Nat. Chem.* **2021**, *13*, 1200–1206.
- (20) Howlett, M. G.; Engwerda, A. H. J.; Scanes, R. J. H.; Fletcher, S. P. An Autonomously Oscillating Supramolecular Self-Replicator. *Nat. Chem.* **2022**, *14*, 805–810.
- (21) Liu, K.; Blokhuis, A.; van Ewijk, C.; Kiani, A.; Wu, J.; Roos, W. H.; Otto, S. Light-Driven Eco-Evolutionary Dynamics in a Synthetic Replicator System. *Nat. Chem.* **2024**, *16*, 79–88.
- (22) Zhang, Y. S.; Khademhosseini, A. Advances in Engineering Hydrogels. *Science* **2017**, *356*, eaaf3627.
- (23) Gentile, K.; Somasundar, A.; Bhide, A.; Sen, A. Chemically Powered Synthetic “Living” Systems. *Chem* **2020**, *6*, 2174–2185.
- (24) Kubota, R.; Hamachi, I. Cell-Like Synthetic Supramolecular Soft Materials Realized in Multicomponent, Non-/Out-of-Equilibrium Dynamic Systems. *Adv. Sci.* **2023**, e2306830.
- (25) Piras, C. C.; Smith, D. K. Self-Propelling Hybrid Gels Incorporating an Active Self-Assembled, Low-Molecular-Weight Gelator. *Chem. Eur. J.* **2021**, *27*, 14527–14534.
- (26) Howard, J.; Hyman, A. A. Growth, Fluctuation and Switching at Microtubule plus Ends. *Nat. Rev. Mol. Cell Biol.* **2009**, *10*, 569–574.
- (27) Alberts, B. *Molecular Biology of the Cell*; Garland Science, 2017.
- (28) Onogi, S.; Shigemitsu, H.; Yoshii, T.; Tanida, T.; Ikeda, M.; Kubota, R.; Hamachi, I. In Situ Real-Time Imaging of Self-Sorted Supramolecular Nanofibres. *Nat. Chem.* **2016**, *8*, 743–752.
- (29) de Jong, J. J. D.; Hania, P. R.; Pugzlys, A.; Lucas, L. N.; de Loos, M.; Kellogg, R. M.; Feringa, B. L.; Duppen, K.; van Esch, J. H. Light-Driven Dynamic Pattern Formation. *Angew. Chem. Int. Ed.* **2005**, *44*, 2373–2376.
- (30) Boekhoven, J.; Hendriksen, W. E.; Koper, G. J. M.; Eelkema, R.; van Esch, J. H. Transient Assembly of Active Materials Fueled by a Chemical Reaction. *Science* **2015**, *349*, 1075–1079.
- (31) Kubota, R.; Makuta, M.; Suzuki, R.; Ichikawa, M.; Tanaka, M.; Hamachi, I. Force Generation by a Propagating Wave of Supramolecular Nanofibers. *Nat. Commun.* **2020**, *11*, 3541.
- (32) van der Weijden, A.; Winkens, M.; Schoenmakers, S. M. C.; Huck, W. T. S.; Korevaar, P. A. Autonomous Mesoscale Positioning Emerging from Myelin Filament Self-Organization and Marangoni Flows. *Nat. Commun.* **2020**, *11*, 4800.
- (33) Kubota, R.; Nagao, K.; Tanaka, W.; Matsumura, R.; Aoyama, T.; Urayama, K.; Hamachi, I. Control of Seed Formation Allows Two Distinct Self-Sorting Patterns of Supramolecular Nanofibers. *Nat. Commun.* **2020**, *11*, 4100.
- (34) Nakamura, K.; Tanaka, W.; Sada, K.; Kubota, R.; Aoyama, T.; Urayama, K.; Hamachi, I. Phototriggered Spatially Controlled Out-of-Equilibrium Patterns of Peptide Nanofibers in a Self-Sorting Double Network Hydrogel. *J. Am. Chem. Soc.* **2021**, *143*, 19532–19541.
- (35) Su, L.; Mosquera, J.; Mabesoone, M. F. J.; Schoenmakers, S. M. C.; Muller, C.; Vleugels, M. E. J.; Dhiman, S.; Wijker, S.; Palmans, A. R. A.; Meijer, E. W. Dilution-Induced Gel-Sol-Gel-Sol Transitions by Competitive Supramolecular Pathways in Water. *Science* **2022**, *377*, 213–218.

- (36) Selmani, S.; Schwartz, E.; Mulvey, J. T.; Wei, H.; Grosvirt-Dramen, A.; Gibson, W.; Hochbaum, A. I.; Patterson, J. P.; Ragan, R.; Guan, Z. Electrically Fueled Active Supramolecular Materials. *J. Am. Chem. Soc.* **2022**, *144*, 7844–7851.
- (37) Barpuzary, D.; Hurst, P. J.; Patterson, J. P.; Guan, Z. Waste-Free Fully Electrically Fueled Dissipative Self-Assembly System. *J. Am. Chem. Soc.* **2023**, *145*, 3727–3735.
- (38) Panja, S.; Adams, D. J. Stimuli Responsive Dynamic Transformations in Supramolecular Gels. *Chem. Soc. Rev.* **2021**, *50*, 5165–5200.
- (39) Sharko, A.; Livitz, D.; De Piccoli, S.; Bishop, K. J. M.; Hermans, T. M. Insights into Chemically Fueled Supramolecular Polymers. *Chem. Rev.* **2022**, *122*, 11759–11777.
- (40) Boekhoven, J.; Brizard, A. M.; Kowgi, K. N. K.; Koper, G. J. M.; Eelkema, R.; van Esch, J. H. Dissipative Self-Assembly of a Molecular Gelator by Using a Chemical Fuel. *Angew. Chem. Int. Ed.* **2010**, *49*, 4825–4828.
- (41) Pappas, C. G.; Sasselli, I. R.; Ulijn, R. V. Biocatalytic Pathway Selection in Transient Tripeptide Nanostructures. *Angew. Chem. Int. Ed.* **2015**, *54*, 8119–8123.
- (42) Tena-Solsona, M.; Rieß, B.; Grötsch, R. K.; Löhner, F. C.; Wanzke, C.; Käsdorf, B.; Bausch, A. R.; Müller-Buschbaum, P.; Lieleg, O.; Boekhoven, J. Non-Equilibrium Dissipative Supramolecular Materials with a Tunable Lifetime. *Nat. Commun.* **2017**, *8*, 15895.
- (43) Leira-Iglesias, J.; Tassoni, A.; Adachi, T.; Stich, M.; Hermans, T. M. Oscillations, Travelling Fronts and Patterns in a Supramolecular System. *Nat. Nanotechnol.* **2018**, *13*, 1021–1027.
- (44) Mishra, A.; Korlepara, D. B.; Kumar, M.; Jain, A.; Jonnalagadda, N.; Bejagam, K. K.; Balasubramanian, S.; George, S. J. Biomimetic Temporal Self-Assembly via Fuel-Driven Controlled Supramolecular Polymerization. *Nat. Commun.* **2018**, *9*, 1295.
- (45) Kumar, M.; Ing, N. L.; Narang, V.; Wijerathne, N. K.; Hochbaum, A. I.; Ulijn, R. V. Amino-Acid-Encoded Biocatalytic Self-Assembly Enables the Formation of Transient Conducting Nanostructures. *Nat. Chem.* **2018**, *10*, 696–703.
- (46) Bal, S.; Das, K.; Ahmed, S.; Das, D. Chemically Fueled Dissipative Self-Assembly That Exploits Cooperative Catalysis. *Angew. Chem. Int. Ed.* **2019**, *58*, 244–247.
- (47) Panja, S.; Adams, D. J. Gel to Gel Transitions by Dynamic Self-Assembly. *Chem. Commun.* **2019**, *55*, 10154–10157.
- (48) Donau, C.; Späth, F.; Sosson, M.; Kriebisch, B. A. K.; Schnitter, F.; Tena-Solsona, M.; Kang, H.-S.; Salibi, E.; Sattler, M.; Mutschler, H.; Boekhoven, J. Active Coacervate Droplets as a Model for Membraneless Organelles and Protocells. *Nat. Commun.* **2020**, *11*, 5167.
- (49) Panja, S.; Dietrich, B.; Adams, D. J. Chemically Fuelled Self - Regulating Gel - to - Gel Transition. *ChemSystemsChem* **2020**, *2*, e190003.
- (50) Singh, N.; Lopez-Acosta, A.; Formon, G. J. M.; Hermans, T. M. Chemically Fueled Self-Sorted Hydrogels. *J. Am. Chem. Soc.* **2022**, *144*, 410–415.
- (51) Jönsson, B.; Lindman, B.; Holmberg, K.; Kronberg, B. *Surfactants and Polymers in Aqueous Solution*; John Wiley & Sons: New York, 2002.
- (52) Horio, T.; Hotani, H. Visualization of the Dynamic Instability of Individual Microtubules by Dark-Field Microscopy. *Nature* **1986**, *321*, 605–607.

